66.7% in high stratum, respectively. These results suggest that in patients with high multimarker score, prognosis is poor and intense follow-up with chest-X ray, echocardiography, and blood examination after discharge is recommended.

Discussion

In the present study, we showed that multimarker score was higher in patients with cardiac events than in those without cardiac events. The univariate Cox proportional hazard analysis demonstrated that patients in the high stratum were associated with the highest risk for cardiac events compared with lower strata. Only multimarker score was an independent predictor of cardiac events among age, NYHA functional class, and LVEF by the multivariate Cox proportional hazard regression analysis. Furthermore, cardiac events occurred most frequently in patients in the high stratum compared with lower strata. These findings suggest that the combination of multiple biomarkers could potentially improve the risk stratification of CHF patients for the prediction of cardiac events.

Our results have clinical importance; incorporating this powerful risk prediction in the management of patients with CHF may be potentially helpful to improve their dismal prognosis. The suggested multiple biomarkers reflecting different aspects of interrelated pathophysiological processes of CHF appear to be suitable to designate this high-risk group of CHF patients. The 7 biomarkers in this study are easy to measure in the routine examination, and can be used multiple times to follow up patients without interobserver variability, and are also appropriate in the emergency setting. Therefore, it seems that this approach using multiple biomarkers is useful as one of the options for risk stratification and information of tailored treatment, which includes more intense monitoring and specialist care in CHF patients.

Many clinicians have encountered problems in CHF patients. How will we identify and detect CHF patients at an earlier stage? How do we predict CHF patients with the greatest risk of cardiac events or cardiac deaths? Shortness of breath, general fatigue, and even edema do not necessarily indicate the presence of CHF in a case. Nevertheless, the clinician must have a high index of suspicion that the source of patients' problems may be CHF and must assess whether patients have volume overload and cardiac dysfunction. It seems that measurement of these 7 markers may aid in the diagnosis and assessment of CHF.

There was no difference in rate of use of ACE inhibitors, ARBs, and β-blockers at discharge among the 3 strata. Multimarker score identified CHF patients who are at increased risk of cardiac events and who may warrant more aggressive therapy. It is important that we perform therapeutic intervention in prospective clinical trials to improve prognosis of severe CHF patients in the future. In addition, patients with preserved ejection fraction were included in this study. We will analyze the difference in multimarker score between patients with preserved ejection fraction and systolic heart failure in the future. Cardiac events increased with advancing multimarker score. Because echocardiography is subject to interobserver variations in interpretation, it seems this multimarker approach is a simple and easy method to estimate severity and prognosis of CHF for many clinicians.

We selected 7 biomarkers on the basis of previous experimental and clinical studies. We acknowledge other biomarkers not tested in this study, such as troponin T or heart-type fatty acid binding protein (markers for ongoing myocardial damage) [13–15], cystatin C (a new marker for renal function) [16], and inflammatory [17] and oxidative stress markers [18]. Improvement in biomarker strategies may depend on the discovery of new biomarkers.

Conclusions

Our findings suggest that this simple multimarker approach demonstrates the potential to assist clinicians in predicting prognosis of CHF patients with low cost and wide availability. Future study is needed to show whether this multimarker approach allows clinicians to improve management and prognosis in CHF patients.

Acknowledgment

This study was supported in part by a grant-in-aid for Scientific Research (No. 19590804) from the Ministry of Education, Science, Sports and Culture, Japan.

References

[1] Funk M, Krumholz HM. Epidemiologic and economic impact of advanced heart failure. J Cardiovasc Nurs 1996; 10:1–10.
[2] Effects of enalapril on mortality in severe congestive heart failure. Results of the Cooperative North Scandinavian

Enalapril Survival Study (CONSENSUS). The CONSENSUS Trial Study Group. N Engl J Med 1987;316:1429–35.
[3] Effect of enalapril on survival in patients with reduced left ventricular ejection fractions and congestive heart failure. The SOLVD Investigators. N Engl J Med 1991;325: 293–302.
[4] Cowburn PJ, Cleland JG, Coats AJ, Komajda M. Risk stratification in chronic heart failure. Eur Heart J 1998;19:696–710.
[5] Berger R, Huelsman M, Strecker K, Bojic A, Moser P, Stanek B, et al. B-type natriuretic peptide predicts sudden death in patients with chronic heart failure. Circulation 2002;105:2392–7.
[6] Anker SD, Doehner W, Rauchhaus M, Sharma R, Francis D, Knosalla C, et al. Uric acid and survival in chronic heart failure: validation and application in metabolic, functional, and hemodynamic staging. Circulation 2003;107:1991–7.
[7] Yin WH, Chen JW, Jen HL, Chiang MC, Huang WP, Feng AN, et al. Independent prognostic value of elevated high-sensitivity C-reactive protein in chronic heart failure. Am Heart J 2004;147:931–8.
[8] Packer M, Lee WH, Kessler PD, Gottlieb SS, Bernstein JL, Kukin ML. Role of neurohormonal mechanisms in determining survival in patients with severe chronic heart failure. Circulation 1987;75:IV80–92.
[9] Ezekowitz JA, McAlister FA, Armstrong PW. Anemia is common in heart failure and is associated with poor outcomes: insights from a cohort of 12 065 patients with new-onset heart failure. Circulation 2003;107:223–5.
[10] McAlister FA, Ezekowitz J, Tonelli M, Armstrong PW. Renal insufficiency and heart failure: prognostic and therapeutic implications from a prospective cohort study. Circulation 2004;109:1004–9.
[11] Guidelines for the evaluation and management of heart failure. Report of the American College of Cardiology/American Heart Association Task Force on Practice Guidelines (Committee on Evaluation and Management of Heart Failure). Circulation 1995; 92:2764–2784.
[12] Richardson P, McKenna W, Bristow M, Maisch B, Mautner B, O'Connell J, et al. Report of the 1995 World Health Organization/International Society and Federation of Cardiology Task Force on the Definition and Classification of cardiomyopathies. Circulation 1996;93:841–2.
[13] Arimoto T, Takeishi Y, Shiga R, Fukui A, Tachibana H, Nozaki N, et al. Prognostic value of elevated circulating heart-type fatty acid binding protein in patients with congestive heart failure. J Card Fail 2005;11:56–60.
[14] Niizeki T, Takeishi Y, Arimoto T, Takahashi T, Okuyama H, Takabatake N, et al. A combination of heart-type fatty acid binding protein and brain natriuretic peptide can reliably risk stratify patients hospitalized for chronic heart failure. Circ J 2005;69:922–7.
[15] Niizeki T, Takeishi Y, Arimoto T, Takabatake N, Nozaki N, Hirono O, et al. Heart-type fatty acid-binding protein is more sensitive than troponin T to detect the ongoing myocardial damage in chronic heart failure patients. J Card Fail 2007;13:120–7.
[16] Arimoto T, Takeishi Y, Niizeki T, Takabatake N, Okuyama H, Fukui A, et al. Cystatin C is a novel predictor of cardiac events in patients with chronic heart failure. J Card Fail 2005;11:595–601.
[17] Suzuki S, Takeishi Y, Niizeki T, Koyama Y, Kitahara T, Sasaki T, et al. Pentraxin 3, a new marker for vascular inflammation, predicts adverse clinical outcomes in patients with heart failure. Am Heart J 2008;155:75–81.
[18] Koyama Y, Takeishi Y, Arimoto T, Niizeki T, Shishido T, Takahashi H, et al. High serum level of pentosidine, an advanced glycation end product (AGE), is a risk factor of patients with heart failure. J Card Fail 2007;13: 199–206.

Journal of Cardiology (2009) 53, 453–457

ELSEVIER

JOURNAL of CARDIOLOGY
Official Journal of the Japanese College of Cardiology
www.elsevier.com/locate/jjcc

CASE REPORT

Complete atrioventricular block due to venous stent migration from innominated vein to right ventricle: A case report

Kazuyoshi Kaneko (MD)[a,*], Osamu Hirono (MD)[b], Kouichi Yuuki (MD)[a], Harutoshi Tamura (MD)[a], Mitsunori Ishino (MD)[a], Hyuuma Daidouji (MD)[a], Hitoshi Ito (MD)[c], Isao Kubota (MD, FJCC)[d]

[a] *Department of Cardiology, Okitama Public General Hospital, 2000 Nishi-otsuka, Kawanishi-machi, Higashi-okitama-gun, Yamagata 992-0601, Japan*
[b] *Department of Cardiology, Yamagata Prefectural Shinjo Hospital, Yamagata, Japan*
[c] *Department of Radiology, Okitama Public General Hospital, Yamagata, Japan*
[d] *Department of Cardiology, Pulmonology, and Nephrology, Yamagata University School of Medicine, Yamagata, Japan*

Received 5 August 2008; received in revised form 29 August 2008; accepted 3 September 2008
Available online 19 October 2008

KEYWORDS
Complete atrioventricular block;
Venous stent;
Stent migration;
Stent retrieve;
Goose-Neck snare catheter

Summary A 78-year-old man who had been treated with maintenance hemodialysis for chronic renal failure was admitted with severe edema in left arm for 1 month. Venous angiography showed a severe stenosis in left innominate vein, then, he underwent percutaneous balloon angioplasty and venous stenting (Wall Stent RP). His arm edema soon improved after angioplasty, however, he complained of general fatigue and bradycardia 2 days after the venous angioplasty. Electrocardiogram showed complete atrioventricular block with 35 wide QRS complexes per minute. His echocardiogram showed a pipe-shaped structure with multiple slit and acoustic shadow in right ventricle. His radiographical right ventriculogram revealed the migrated venous stent from innominate vein to right ventricle. We tried to perform percutaneous transvenous stent extraction using Goose-Neck snare catheter, however, the wall stent stuck in the right external iliac vein, and contrast media leaked to the outside of the vascular wall. Therefore, we implanted this stent in the iliac vein with optimal-sized balloon inflation, and succeeded in stopping bleeding. Complete atrioventricular block was recovered to sinus rhythm with left bundle branch block just after the removal of the venous stent from right ventricle, and no cardiovascular events occurred after the treatment.

* Corresponding author. Tel.: +81 234 26 2001; fax: +81 234 26 5114.
E-mail address: kzkaneko@nihonkai.gr.jp (K. Kaneko).

0914-5087/$ – see front matter © 2008 Japanese College of Cardiology. Published by Elsevier Ireland Ltd. All rights reserved.
doi:10.1016/j.jjcc.2008.09.001

Introduction

It has been reported that transient atrioventricular block is caused by mechanical and physiological disorders such as trauma, myocardial ischemia, infection, neurally mediated and/or metabolic diseases, and iatrogenic injury of the atrioventricular node (catheter, radiofrequency energy, surgical procedure, and drug-induced) [1].

It is well known that dislodgement and/or migration of the intravascular stent are major complications in radiological intervention [2–7], however, there are few reports regarding stent migration from innominate vein to intra-cardiac cavity causing transient and complete atrioventricular block.

Percutaneous transvascular stent extraction using Goose-Neck snare catheter is thought to be a useful procedure to retrieve it [3,6,8,9]. Although Goose-Neck snare catheter is a popular procedure for stent extraction, we experienced stent sticking in the external iliac vein and vascular rupture. Herein, we report the intracardiac migration of the vascular stent and the pitfall of using percutaneous stent extraction.

Case report

A 78-year-old man who had been treated with maintenance hemodialysis for 2 years due to chronic renal failure was admitted with severe edema in his left arm, which had an arterio-venous shunt for dialysis, for 1 month. His venous angiography showed a severe stenosis in left innominate vein, then, he underwent percutaneous balloon angioplasty (Synergy balloon catheter, Boston Scientific, Natick, MA, USA; 10 mm in diameter and 4.0 cm in length) and venous stent implantation (Wall Stent RP, Boston Scientific; 10 mm/3.9 cm). Although his arm edema soon improved after angioplasty, he complained of general fatigue and bradycardia 2 days after the venous angioplasty. His electrocardiogram showed left bundle branch block with sinus rhythm on admission, and complete atrioventricular block with 35 wide QRS complexes per minute 2 days after the operation. He did not receive oral administration of anti-arrythmic medicine, and circulating levels of electrolyte, including sodium, potassium, and magnesium levels, were normal. His echocardiogram showed global reduced motion and eccentric hypertrophy in left ventricle (60 mm in left ventricular end-diastolic dimension and 30% in fractional shortening) and a pipe-shaped structure

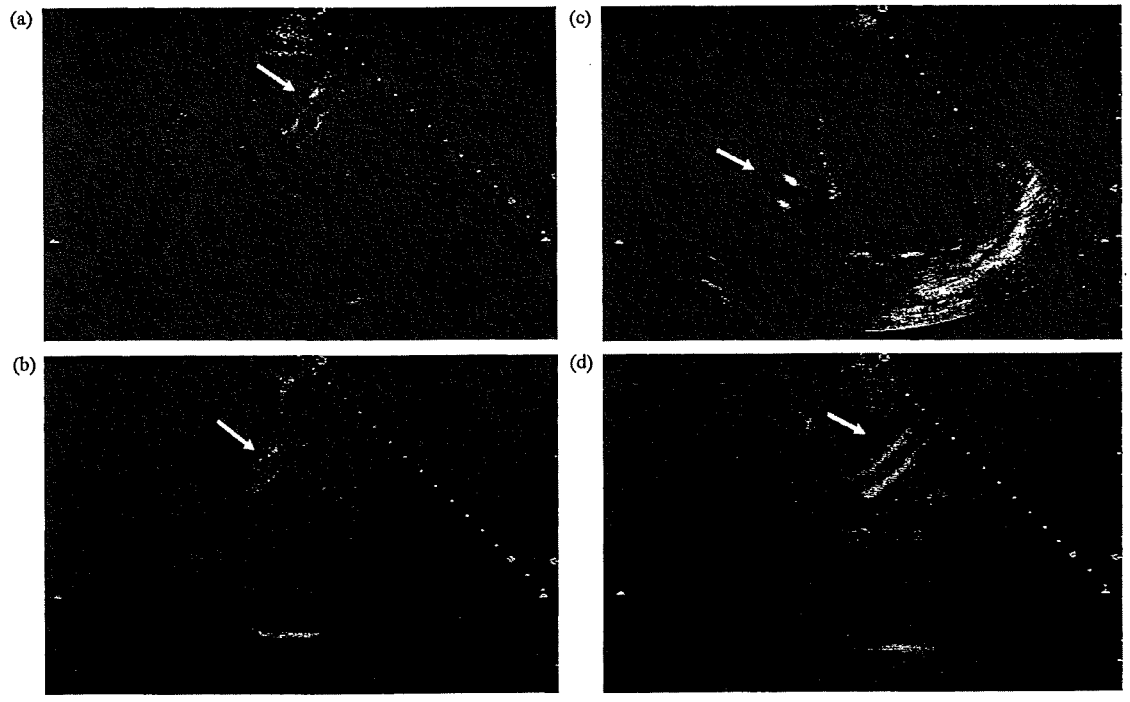

Figure 1 B-mode echocardiograms showing pipe-shaped structure with multiple slit and acoustic shadow (arrows) in right ventricle: (a) parasternal long-axis view; (b) parasternal short-axis view; (c) apical four-chamber view; (d) apical short-axis view.

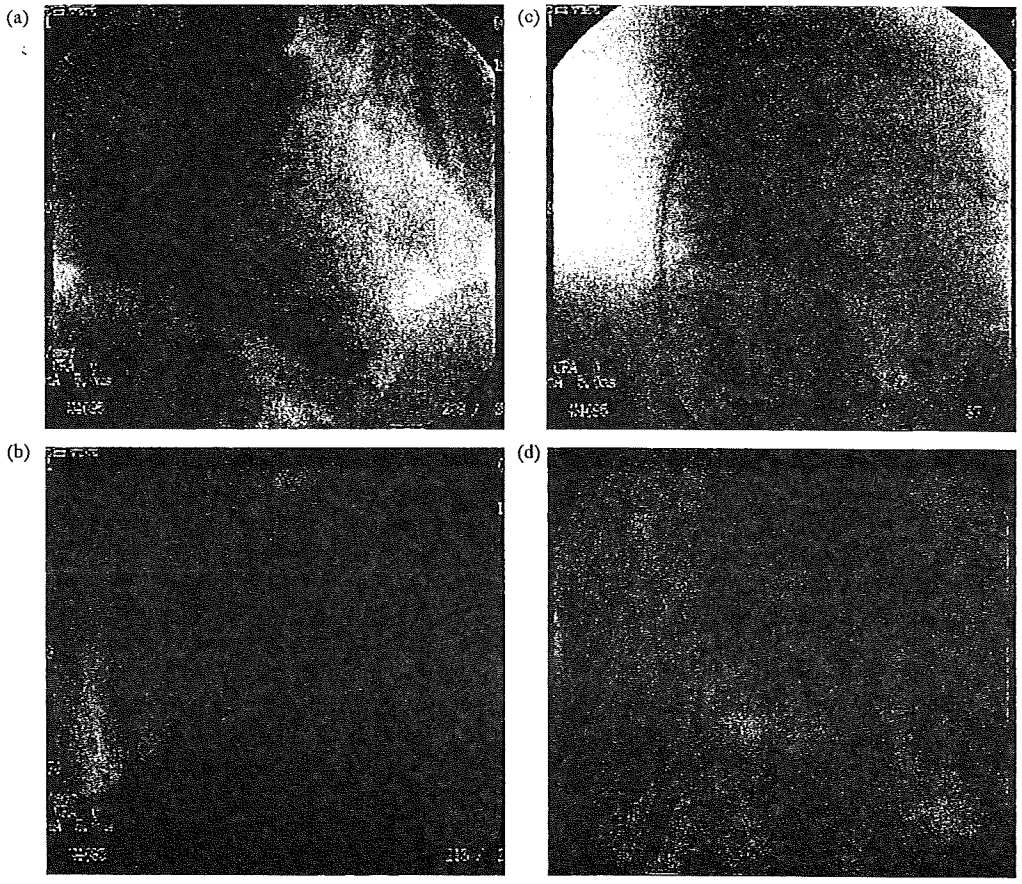

Figure 2 Right ventriculograms showing migrated venous stent in the right ventricle (a and b), and percutaneous transvenous stent extraction using Goose-Neck snare catheter (c and d). (a) RAO view; (b) LAO view; (c) stent retrieval from right ventricular cavity; (d) stent lodging in the right internal iliac vein.

with multiple slit and acoustic shadow in right ventricle (Fig. 1). He was transported to the catheter laboratory without delay, and underwent right ventricular temporary pacing. His radiographical right ventriculogram revealed the migrated venous stent between basal free and septal wall in the right ventricle (Fig. 2a and b). We did not select surgical removal of the venous stent because he had complications with renal failure and severe left ventricular dysfunction. We tried to perform percutaneous transvenous stent extraction using 6Fr Amplatz Goose-Neck snare catheter (C. R. Bard, Inc. USA) with 14Fr sheath introducer (Medikit, Tokyo, Japan) from right femoral vein (Fig. 2c and d). Although we succeeded in retrieving the stent from right ventricular cavity using this catheter, the wall stent stuck in the right external iliac vein, and contrast media leaked to the outside of the vascular wall while trying to catch and retrieve this stent through the venous sheath using a T-REX biotome catheter for the ventricular biopsy (Boston Scientific) (Fig. 3a). Therefore, we implanted this stent in the iliac vein with optimal-sized balloon inflation (Synergy balloon catheter, Boston Scientific; 10 mm/7.5 cm), and succeeded in stopping bleeding (Fig. 3). Complete atrioventricular block was recovered to sinus rhythm with left bundle branch block just after the removal of the venous stent from right ventricle, and no cardiovascular events occurred after the treatment.

Discussion

We experienced a case with venous stent migration into the right ventricular cavity causing transient atrioventricular block, and iliac venous wall rupture when performing stent extraction using Amplatz Goose-Neck snare catheter.

In the present case, we did not choose open-heart surgery and stent extraction. We thought that open-heart surgery with artificial cardiopulmonary

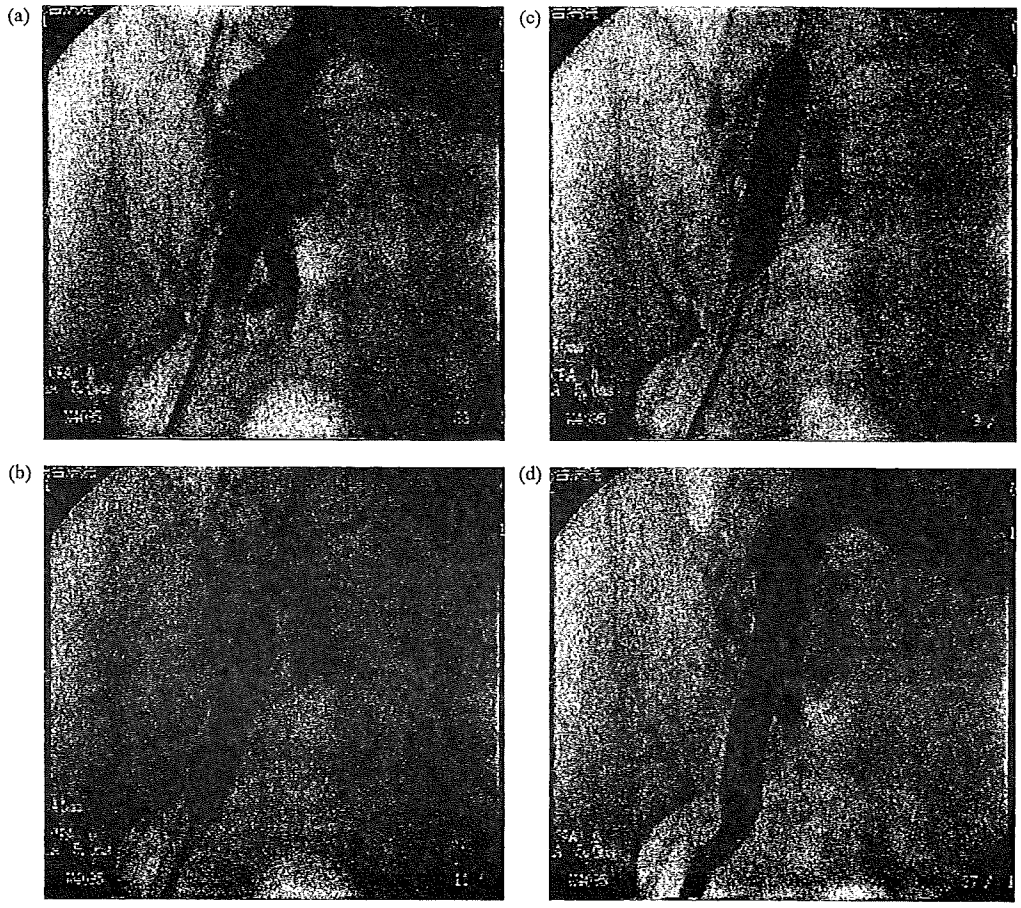

Figure 3 Radiographic angiograms showing contrast media leaked to the outside of the right external iliac vein (a), stent implantation and optimal-sized balloon inflation in the iliac vein (b and c), and after the balloon angioplasty (d).

bypass would be associated with a high risk of cardiovascular complications. This patient had renal failure and left ventricular dysfunction that seemed to be the dilated phase of end-stage hypertensive heart disease, because the patients' pathogenesis of chronic renal failure had been suspected to be renal sclerosis due to hypertension. Furthermore, we had to remove the venous stent as soon as possible because this patient had a symptomatic complete atrioventricular block. As a result, we succeeded in stent extraction by percutaneous and transvenous approach, and atrioventricular block was recovered to sinus rhythm.

It has been previously reported that a vascular stent was implanted to superior vena cava to improve superior vena cava syndrome [10]. These reports suggest that stent migration into the right atrium and/or ventricle by the stenting in the venous system has potentially fatal complications such as arrhythmias, thrombus, and/or infections, and is most likely to occur during the treatment of superior vena cava obstruction [5–7]. Furthermore, it has been reported that cardiac tamponade occurred by migrated inferior vena cava filter implanted for a case with deep venous thrombosis [11]. In our experience, it is thought to be rare that the vascular stent implanted in the left innominate vein migrated to the right ventricle and caused transient and complete atrioventricular block. It is speculated that vascular stents might be liable to migrate in the venous system as compared to the arterial system that has intimal proliferation and comprehension.

Migration and/or dislodgement of coronary stents sometimes occurred and were retrieved with balloon catheters, guide wires, guiding catheters, and direct snaring [3–6]. In the present case, we used Amplatz Goose-Neck snare catheter to retrieve migrated venous stents according to a few previous reports [3,6,8,9]. Although we succeeded in retrieving the stent from the right ventricular cavity using this catheter, the wall stent stuck

in the right external iliac vein and vascular rupture occurred. The wall stent is a self-expanding stent, therefore, stent diameter in the present case might be larger than 14Fr venous sheath introducer catheter in spite of using this sheath as large lumen as possible. On the other hand, it might be useful to implant migrated stent in the sticking site using optimal-sized balloon inflation to stop bleeding and repair venous rupture [12].

Venous thrombosis, pulmonary embolism, and complete atrioventricular block without anti-coagulant therapy have not occurred for 2 years. Three years passed from the implantation of venous stent, and he has received anti-coagulant therapy for persistent atrial fibrillation.

We have reported here a case of self-expanding stent migration from innominate vein into right ventricle that caused transient and complete atrioventricular block. We used Amplatz Goose-Neck snare catheter and succeeded to retrieve the migrated venous stent from right ventricle, however, the stent stuck in the iliac vein and caused vascular rupture. Further experience is required to retrieve the migrated venous stent safely and quickly.

References

[1] Kayano H, Ueda H, Kawamata T, Miyoshi F, Toshida T, Watanabe N, Hirano Y, Kawamura M, Asano T, Kou S, Tanno K, Ozawa M, Kobayashi Y, Katagiri T. Improved septal contraction and coronary flow velocity after cardiac resynchronization therapy elucidated by strain imaging and pulsed wave Doppler echocardiography. J Cardiol 2006;47:51–61.

[2] Eeckhout E, Stauffer JC, Goy JJ. Retrieval of a migrated coronary stent by means of an alligator forceps catheter. Cathet Cardiovasc Diagn 1993;30:166–8.

[3] Kobayashi Y, Nonogi H, Miyazaki S, Daikoku S, Yamamoto Y, Takamiya M. Successful retrieval of unexpanded Palmaz-Schatz stent from left main coronary artery. Cathet Cardiovasc Diagn 1996;38:402–4.

[4] Meisel SR, DiLeo J, Rajakaruna M, Pace B, Frankel R, Shani J. A technique to retrieve stents dislodged in the coronary artery followed by fixation in the iliac artery by means of balloon angioplasty and peripheral stent deployment. Cathet Cardiovasc Interv 2000;49:77–81.

[5] Srinathan S, McCafferty I, Wilson I. Radiological management of superior vena caval stent migration and infection. Cardiovasc Intervent Radiol 2005;28:127–30.

[6] Taylor JD, Lehmann ED, Belli AM, Nicholson AA, Kessel D, Robertson IR, Pollock JG, Morgan RA. Strategies for the management of SVC stent migration into the right atrium. Cardiovasc Intervent Radiol 2007;30:1003–9.

[7] Poludasu SS, Vladutiu P, Lazar J. Migration of an endovascular stent from superior vena cava to the right ventricular outflow tract in a patient with superior vena cava syndrome. Angiology 2008;59:114–6.

[8] Koseoglu K, Parildar M, Oran I, Memis A. Retrieval of intravascular foreign bodies with goose neck snare. Eur J Radiol 2004;49:281–5.

[9] Bui JT, West DL, Pinto C, Gramling-Babb P, Owens CA. Right ventricular migration and endovascular removal of an inferior vena cava filter. J Vasc Interv Radiol 2008;19:141–4.

[10] Qanadli SD, El Hajjam M, Mignon F, de Kerviler E, Rocha P, Barré O, Chagnon S, Lacombe P. Subacute and chronic benign superior vena cava obstructions: endovascular treatment with self-expanding metallic stents. Am J Roentgenol 1999;173:159–64.

[11] Saeed I, Garcia M, McNicholas K. Right ventricular migration of a recovery IVC filter's fractured wire with subsequent pericardial tamponade. Cardiovasc Intervent Radiol 2006;29:685–6.

[12] Funatsu A, Shibata K, Yamamoto R, Ono T, Mizobuchi M, Yokouchi I, Kanbayashi D, Kobayashi T, Enjoji Y, Nakamura S. Initial and long term outcomes of stent implantation for iliac compression syndrome. J Cardiol 2007;50:371–7.

Original Article

Deficiency of Clusterin Inhibits Neointimal Hyperplasia After Vascular Injury

Takahiro Shirasawa[1], Masaaki Miyata[1], Hideyuki Eto[1], Narisato Hamada[1], Yuichi Akasaki[1], Takahiro Miyauchi [1], Yuko Furusho[1], Koji Orihara[1], Shuichi Hamasaki[1], Bruce J. Aronow[2], Jonathan D. Smith[3], and Chuwa Tei[1]

[1]Department of Cardiovascular, Respiratory and Metabolic Medicine, Graduate School of Medicine, Kagoshima University, Kagoshima, Japan
[2]Cincinnati Children's Hospital Medical Center, Cincinnati, OH, USA
[3]Department of Cell Biology, The Cleveland Clinic, Cleveland, OH, USA

Aim: Increased clusterin mRNA and protein levels have been detected in various tissues undergoing stress, and we previously reported that clusterin is markedly induced in media and neointima following vascular injury. The present study therefore investigated the impact of clusterin on neointimal hyperplasia following vascular injury.
Methods and Results: As compared with wild-type mice, clusterin knockout mice (clusterin-KO) demonstrated a significant decrease of the intima/media ratio 4 weeks after cuff placement. Immunohistochemical analysis of injured femoral arteries in clusterin-KO demonstrated the accumulation of p53 in nuclei of neointimal vascular smooth muscle cells (VSMCs). Moreover, VSMCs from either clusterin-KO or rat VSMCs treated with clusterin-short-interfering (si) RNA subjected to static stretch exhibited significantly increased p53 and p21, and increased G1 cell cycle arrest as indicated by flow cytometry compared with VSMCs from wild-type mice.
Conclusion: Reduced clusterin expression reduced the proliferation of VSMCs and induced G1 arrest via p53 and p21. Clusterin therefore represents a promising molecular target to limit restenosis after coronary intervention.

J Atheroscler Thromb, 2009; 16:772-781.

Key words; Clusterin, p53, p21, Vascular smooth muscle cell, Neointima

Introduction

Percutaneous coronary intervention (PCI) is a useful procedure for the treatment of coronary stenosis. Sirolimus-eluting and polymeric paclitaxel-eluting stents strongly suppress neointimal hyperplasia[1-3]; however, meta-analysis of randomized clinical trials of drug-eluting stents reported that the rate of angiographic restenosis after drug-eluting stents is 8.9%[4]. Thus, restenosis after PCI is still a significant problem. Identifying the molecules involved in restenosis after PCI will help to develop new strategies for the prevention of restenosis. Neointimal hyperplasia is a major cause of restenosis after PCI[5]. We previously reported that clusterin was markedly induced in media and neointima following vascular injury, and the expression of clusterin stimulated the proliferation and migration of cultured vascular smooth muscle cells (VSMCs) *in vitro*[6]. Moreover, clusterin antisense was reported to inhibit the proliferation of cultured VSMC obtained from neointima after ballooning *in vitro*[7]; however, it is unknown whether clusterin stimulates or protects against restenosis following vascular injury *in vivo*.

Clusterin, also known as apolipoprotein J, testosterone-repressed prostate message-2, or sulphated glycoprotein-2, is a secretory heterodimetric disulphide-

Address for correspondence: Masaaki Miyata, Department of Cardiovascular, Respiratory and Metabolic Medicine, Graduate School of Medicine, Kagoshima University, 8-35-1 Sakuragaoka, Kagoshima 890-8520, Japan
E-mail: miyatam@m3.kufm.kagoshima-u.ac.jp
Received: February 27, 2009
Accepted for publication: May 19, 2009

linked glycoprotein (449 amino acids) that is expressed in virtually all tissues and is found in most physiological fluids, including human plasma, urine, breast milk, semen, and cerebrospinal fluid[8, 9]. The wide distribution and sequence conservation of clusterin suggests that this protein performs functions of fundamental biological importance. It is involved in numerous physiological processes important for carcinogenesis and tumor growth, including apoptotic cell death, cell-cycle regulation, DNA repair, cell adhesion, tissue remodeling, lipid transportation, membrane recycling, and immune system regulation. Increased clusterin mRNA and protein levels have been consistently detected in various tissues after stress, including the heart, brain, liver, kidney, breast, and retinal tissues both *in vivo* and *in vitro*[10].

The purpose of this study was to investigate the impact of clusterin on neointimal hyperplasia following vascular injury *in vivo*, and to clarify the precise mechanism of the effect of clusterin on the proliferation of VSMC *in vitro*.

Materials and Methods

Mice

This study was performed under the supervision of the Animal Research Committee in accordance with the guidelines on animal experiments of the Faculty of Medicine, Kagoshima University. We used C57BL6 (wild-type) and clusterin knockout mice (clusterin-KO) in this study. Clusterin-KO mice were as described by McLaughlin *et al.*[11]. We used 8-week-old male mice that weighed 24–30 g. The animals were given a standard diet and water ad libitum. In order to confirm the deficiency of clusterin, mice tails were biopsied at 8 weeks of age. Genomic DNA was isolated using proteinase K and analyzed with the polymerase chain reaction as described.

Cuff Placement

Neointimal formation in the femoral artery of mice was induced by placement of a polyethylene cuff as described previously[12, 13]. Mice were anesthetized with pentobarbital (50 mg/kg) by intraperitoneal injection and diethyl ether. The right femoral artery of the mouse was exposed and isolated from the surrounding tissues. A non-constrictive polyethylene cuff (length, 2.0 mm; inner diameter, 0.40 mm; outer diameter, 0.80 mm; Natsume, Tokyo, Japan) was cut longitudinally and loosely placed around the right femoral artery and tied in place with an 8-0 silk suture. The cuff was larger than the vessel and did not obstruct blood flow. The left femoral artery was dissected from the surrounding tissue, but a cuff was not placed (sham-operated). The wounds were closed with sutures.

Tissue Harvesting and Lipid Analysis

Four weeks after cuff placement, the mice were killed by an overdose of pentobarbital. For morphometric analysis, the thorax was opened, and blood samples were taken through a 23-gauge butterfly angiocatheter placed in the left ventricle. Subsequently, the mice were perfused with PBS, and the vessels were perfusion-fixed at 100 mmHg with 10% neutral-buffered formalin. The cuffed artery and sham-operated artery were harvested and then postfixed in 10% neutral-buffered formalin overnight and embedded in paraffin.

The concentration of plasma total cholesterol and high density lipoprotein (HDL) cholesterol was measured enzymatically using a commercially available kit (Kainos Laboratories, Tokyo, Japan).

Morphometric Analysis

The artery was cut into three subserial cross sections of 10 μm thickness at intervals of 0.5 mm. The sections were stained by hematoxylin and eosin (H&E) and Elastica van Gieson, and photographed with a microscale. The areas of the media and neointima were measured using image analyzing software (NIH image) by an observer blinded to the animal's genotype. Neointima was defined as the area between the vessel lumen and the internal elastic lamina. Media was defined as the area between the internal elastic lamina and the external elastic lamina. We also calculated the intima-to-media ratio (I/M ratio) of each section. The average value of these sections was taken as the value for each animal.

Immunohistochemistry

Immunohistochemical staining of the tissue sections was performed as described previously[6] by the labeled streptavidin-biotin complex method (Nichirei Bioscience, Tokyo, Japan). A goat polyclonal antibody against human apoJ (Rockland Immunochemicals, Gilbertsville, PA), a goat polyclonal antibody against human p53 (Santa Cruz Biotechnology, Santa Cruz, CA), a rabbit polyclonal antibody against human activated caspase-3 (BD Bioscience, Franklin Lakes, NJ), and a rabbit polyclonal antibody against human p21 (Santa Cruz Biotechnology) were used as primary antibodies. The specificity of the immunoreaction was evaluated in comparison with a negative control specimen in which goat or rabbit IgG was used instead of the primary antibody.

VSMC Isolation from Clusterin-KO and Wild-Type Mice

VSMCs were isolated by an explant method from the medial layer of the thoracic aorta obtained from clusterin-KO or wild-type mice. VSMCs were cultured in DMEM containing 5% FBS in a humidified atmosphere and 5% CO_2–95% air as described previously[14]. VSMCs from the fifth to tenth passage were used in the experiments. The identity of cultured VSMC was confirmed by microscopic identification of their characteristic "hill-and-valley" growth pattern and by immunohistochemical identification of smooth muscle actin using a specific monoclonal antibody (human α-actin; Santa Cruz Biotechnology).

Static Stretch System

The strain unit, Flexcell FX-2000 (Flexcell International, Hillsborough, NC), consists of a vacuum unit linked to a valve controlled by a computer program. VSMCs cultured on the flexible membrane base were subjected to static stretch produced by this computer-controlled application of sinusoidal negative pressure as described previously[15, 16]. Flex I culture plates not subjected to static stretch served as controls.

Proliferation Assay of VSMC with or without Stretch

VSMCs from wild-type or clusterin-KO mice were cultured on Flex I 6-well plates coated with type-I collagen (density, 2×10^5/well) with medium containing 5% FBS. After 48 h, VSMCs were exposed to static stretch provided by 25% radial stretch of the membrane for 10 min. After 48 h with or without stretch, we demonstrated VSMC proliferation by counting cells with an electronic counter (Sysmex, Hyogo, Japan).

In addition, after 24 h with or without stretch, we used VSMCs for Western blotting and cell-cycle analysis by flow cytometry.

Western Blotting

For Western blotting of clusterin, p53, p21, cleaved caspase-3, and α-actin, proteins were extracted from cultured VSMCs of clusterin-KO mice, wild-type mice, and rat aorta as reported previously[17, 18]. Cells were incubated in ice-cold 0.1% Triton lysis solution [mmol/L: HEPES 10 (pH 7.4), sodium pyrophosphate 50, NaF 50, EDTA 5, EGTA 5, and NaCl 50, and 100 mmol/L Na_3VO_4, 0.1% Triton X-100, 500 mmol/L PMSF, and 10 mg/mL leupeptin] for 1 h.

Insoluble matter was removed by centrifugation, and the protein concentration was measured by a bicinchoninic acid assay (PIERCE Biotechnology, Rockford, IL). Western blotting was performed with a NuPAGE Electrophoresis System (Invitrogen, Carlsbad, CA) as reported previously[19]. Briefly, protein samples were resuspended in reduced sample buffer, electrophoresed on a 4–12% Bis-Tris gel (Invitrogen) with MOPS running buffer, blotted to a PVDF membrane (Millipore, Billerica, MA), and sequentially probed with a goat polyclonal antibody against mouse clusterin, a mouse monoclonal antibody against human p53, a rabbit polyclonal antibody against human p21, a rabbit polyclonal antibody against human cleaved caspase-3, and a mouse monoclonal antibody against human α-actin (all from Santa Cruz Biotechnology). Either horseradish peroxidase-conjugated goat anti-mouse antibody, goat anti-rabbit antibody, or donkey anti-goat antibody (all from Santa Cruz Biotechnology) was then added, and the secondary antibody was detected by autoradiography using enhanced chemiluminescence (GE Healthcare, Little Chalfont, England). The expression of α-actin was used as a reference for quantification of the respective proteins. Densitometric analysis was performed to quantitate the protein expression of clusterin, p53, p21, and α-actin using NIH image software. The α-actin protein was used as a reference for quantitation of clusterin, p53, and p21.

Flow Cytometry for Cell Cycle Analysis

The cell cycle was assessed by flow cytometry (Beckmann Coulter, Fullerton, CA). VSMCs were fixed with 70% ethanol on ice for 30 min, washed with phosphate-buffered saline (PBS), treated with RNase A (100 μg/mL) for 30 min at 37℃ and stained for DNA with propidium iodide (10 μg/mL) for 15 min at room temperature. Cells were centrifuged, resuspended in 1 mL PBS, and analyzed using flow cytometry as described previously[20].

Short-Interfering RNA Transfection and Stretch of Rat VSMCs

We used short-interfering (si) RNA to suppress the expression of clusterin. The sequences of siRNA against clusterin (clusterin-siRNA) were 5'-GGCUUUCCCGGAAGUGUGUdtdt-3' (sense) and 5'-ACACACUUCCGGGAAAGCCdtdt-3' (antisense). These siRNA and negative control siRNA (control-siRNA), a 21-nucleotide RNA duplex with no known sequence homology[21], were purchased from Ambion (Austin, TX). For siRNA transfection, rat VSMCs were cultured on Flex I 6-well plates coated with type-I collagen (density, 4×10^4/well) with medium containing 10% FBS. After reaching 50–60% confluence, transfection of siRNA into rat VSMCs was achieved using oligofectamine (Invitrogen). Briefly, 20 μmol/L stock

siRNA and 8 μL oligofectamine were diluted and mixed gently with 1 mL M199 to achieve the final concentration of oligofectamine, 8 μL/well. Cultured cells were washed with M199 without serum and antibiotics. The oligonucleotide-oligofectamine complexes were then added to each well and the cells were incubated at 37℃ for 4 h. FBS was then added to the cells to achieve a final concentration of 5% in M199 and incubated for 2 h. The cells were then exposed to static stretch provided by 25% radial stretch of the membrane for 10 min. Twenty-four hours after stretching, total RNA was isolated from cultured VSMCs for reverse-transcription polymerase chain reaction (RT-PCR). Forty-eight hours after stretching, we analyzed the cell number and isolated protein for Western blotting as described previously[22].

RT-PCR

RT-PCR was performed as described previously[17]. Total RNA for use in RT-PCR was isolated using the Mini RNA isolation kit (ZYMO RESEARCH, Orange, CA). For cDNA synthesis, 0.5 μg total RNA was reverse-transcribed with random hexamers using SuperScript II RT (Invitrogen). The transcribed cDNA was amplified by PCR with specific primers for clusterin and glyceraldehydes-3-phosphate dehydrogenase (GAPDH). Two specific primer pairs corresponding to published sequences were used to amplify clusterin (5'-TGATGGCCCTCTGGGAAGAGT-3' and 5'-TCTCCAGCAGGGAGTCGATGCG-3')[23] and GAPDH (5'-ATGGTGAAGGTCGGTGTG-3' and 5'-ACCAGTGGATGCAGGGAT-3')[24]. The PCR amplification protocol included 31 cycles of denaturing, annealing, and elongation with Taq polymerase (TaKaRa Bio, Shiga, Japan). Equal amounts of PCR products were subjected to electrophoresis through 2% agarose gels and visualized with ethidium bromide. GAPDH expression was used as a reference.

Statistical Analysis

All calculated data are presented as the mean ± S.D. and analyzed by unpaired Student's t test. A value of $p<0.05$ was considered significant.

Results

Mice

To clarify the impact of clusterin on vascular remodeling, we compared wild-type mice with clusterin-KO mice.

We measured the body weight and plasma level of total cholesterol and HDL cholesterol in wild-type and clusterin-KO mice at 12 weeks of age and found no significant difference (**Fig. 1**).

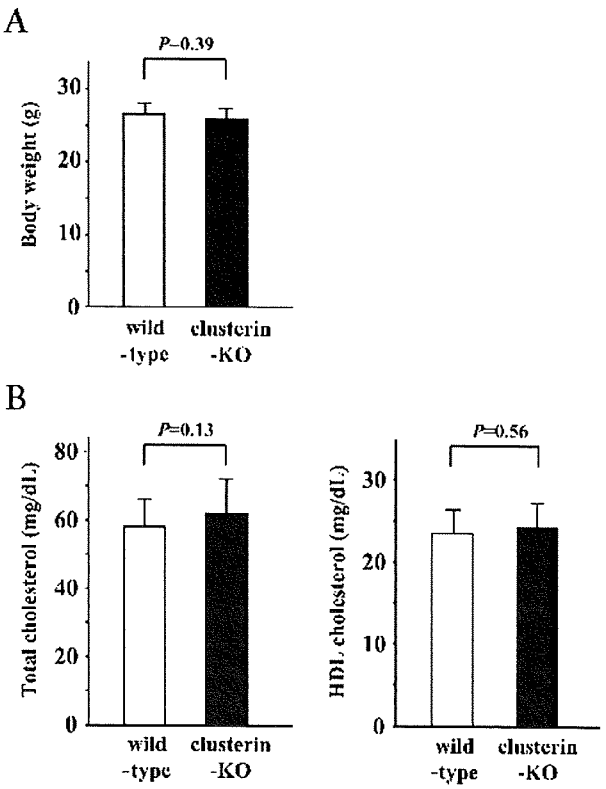

Fig. 1. Body weight (A) and plasma levels of total cholesterol and HDL cholesterol (B) in wild-type (white bar) and clusterin-KO mice (black bar) ($n=15$ mice per group) at 12 weeks of age.

There was no significant difference in the body weight, plasma levels of total cholesterol and HDL cholesterol between wild-type and clusterin-KO.

Quantification of Intimal Lesions After Cuff Placement

We quantified morphometric changes in the injured artery of wild-type and clusterin-KO mice 4 weeks after cuff placement. There was no significant difference in the medial area between wild-type and clusterin-KO mice (**Fig. 2A, B**); however, clusterin-KO mice demonstrated a significant decrease of the I/M ratio ($p<0.01$) as compared with wild-type mice (**Fig. 2C**).

Analysis of Proliferation and Apoptosis of VSMCs in Intimal Lesions

In order to analyze the mechanism of the effect of clusterin deficiency on neointimal formation following vascular injury, we performed immunohistochemical staining using anti-p53 antibody. In clus-

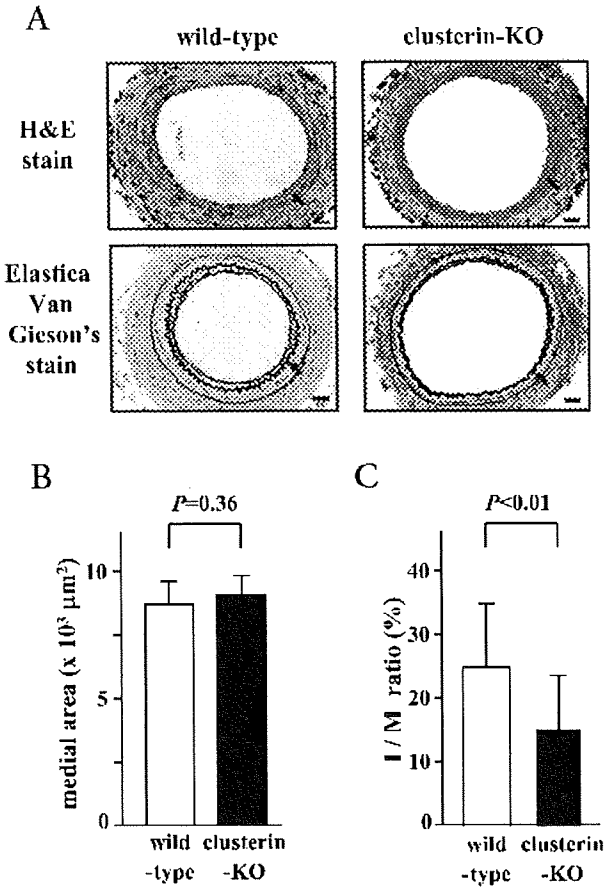

Fig. 2. Clusterin-KO mice showed a significant decrease in the I/M ratio.

Representative sections of the injured femoral artery from wild-type and clusterin-KO mice 4 weeks after cuff placement, stained by H&E and Elastica Van Gieson (A). Arrows indicate internal elastic lamina. Quantification of the medial area (B) and the I/M ratio (C) of the injured femoral artery 4 weeks after cuff placement in wild-type (white bar) and clusterin-KO (black bar) ($n=15$ mice per group). There is no significant difference in the medial area between wild-type and clusterin-KO; however, clusterin-KO mice showed a significant decrease in the I/M ratio. All scale bars denote 25 μm.

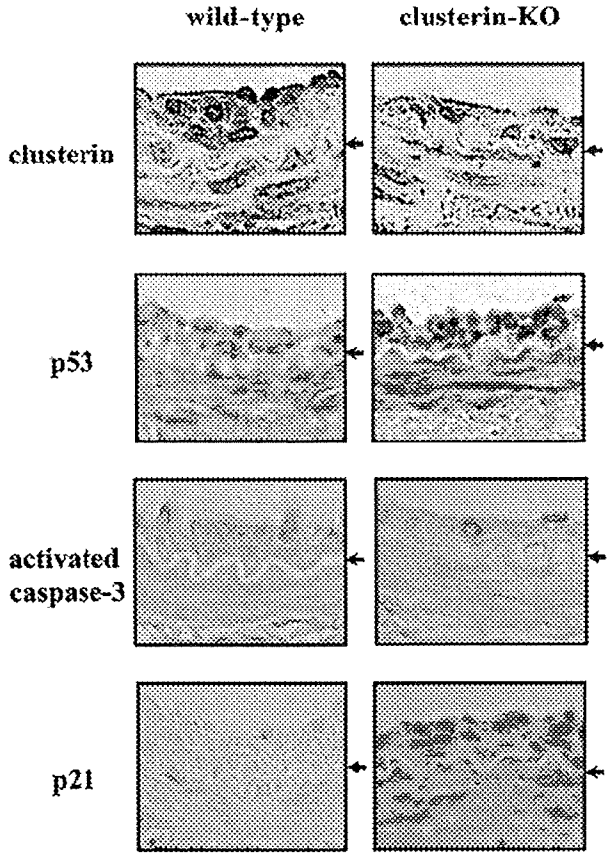

Fig. 3. Clusterin-KO mice demonstrated accumulation of p53 and p21 in nuclei of neointimal VSMCs in injured arteries.

Immunohistochemical staining of clusterin, p53, activated caspase-3, and p21 in the injured femoral artery 4 weeks after cuff placement from wild-type and clusterin-KO mice. Arrows indicate internal elastic lamina.

terin-KO mice, the accumulation of p53 in the nuclei of neointimal VSMCs was detected (**Fig. 3**). This result suggested that apoptosis or G1 arrest occurred in neointimal VSMCs of clusterin-KO mice. Furthermore, we examined apoptosis using anti-activated caspase-3 antibody, and the immunoreactivity of activated caspase-3 in neointima demonstrated no differences between wild-type and clusterin-KO mice (**Fig. 3**). We then performed immunohistochemistry on p21 to analyze G1 arrest of neointimal VSMCs. In clusterin-KO mice, p21 was accumulated in the nuclei of neointimal VSMCs (**Fig. 3**), suggesting that G1 arrest occurred in neointimal VSMCs of clusterin-KO mice.

Proliferation Stimulated by Stretching in VSMCs Obtained from Clusterin-KO or Wild-Type Mice

VSMCs were explanted from the thoracic aorta obtained from clusterin-KO or wild-type mice. The cell number and protein expression of clusterin in wild-type VSMCs increased with the strength of stretch (**Fig. 4**), and therefore, we decided to use the maximum 25% stretch for 10 min in this experiment. **Fig. 5A** demonstrates the fold increase of cell number after 48 h with or without 25% stretch for 10 min in wild-type and clusterin-KO VSMCs. Wild-type VSMCs showed a significant 1.2-fold increase of cell number by stretching, but clusterin-KO VSMCs did not.

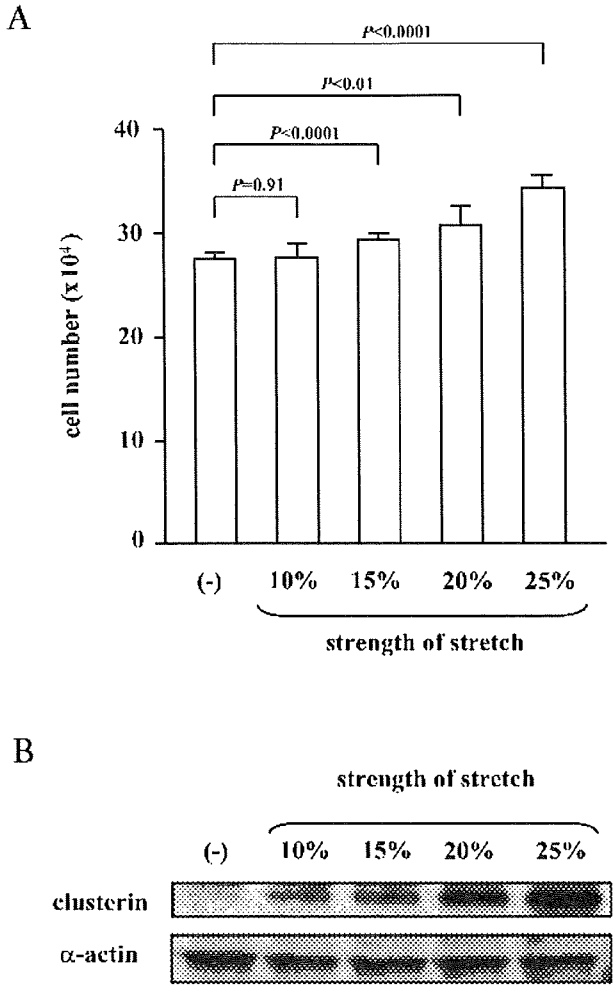

Fig. 4. Cell number (A) ($n=3$ per group) and protein expression of clusterin (B) in wild-type VSMCs increased with the strength of stretching.

Induction of p53 and p21 by Stretching in Clusterin-KO VSMCs

Cultured VSMCs of clusterin-KO and wild-type mice were exposed to 25% static stretch for 10 min. After 24 h, the expressions of clusterin, p53, and p21 were analyzed by Western blot analysis. Clusterin was induced by 25% static stretch in wild-type VSMCs, but not in clusterin-KO VSMCs. In addition, the expression of p53 and p21 was induced by 25% static stretch in clusterin-KO VSMCs, but not in wild-type VSMCs (**Fig. 5B**).

Cell Cycle Analysis

Next, cell cycle was analyzed by flow cytometry 24 h after 25% static stretch for 10 min. As shown in **Fig. 5C**, there was a significant progression to S and G2/M phases in clusterin-KO VSMCs compared with wild-type VSMCs 24 h after stretching, suggesting G1 arrest in clusterin-KO VSMCs (wild-type VSMCs: G0/G1 70.7 ± 1.8%, S 6.4 ± 1.8%, G2/M 21.8 ± 1.7%, sub-G1 1.5 ± 0.3% vs. clusterin-KO VSMCs: G0/G1 86.2 ± 4.3%, S 3.9 ± 1.0%, G2/M 8.2 ± 3.0, sub-G1 1.3 ± 0.7%).

Induction of Clusterin by Static Stretch and Knock Down by siRNA in Rat VSMCs

We analyzed the expression of clusterin in rat VSMCs transfected with control or clusterin-siRNA at 24 h after 25% stretch for 10 min. RT-PCR demonstrated that the expression of clusterin was upregulated by stretching in rat VSMCs. We confirmed that clusterin-siRNA but not control-siRNA inhibited the expression of clusterin mRNA induced by stretching (**Fig. 6A**).

Clusterin-siRNA Decreased VSMC Proliferation Stimulated by Static Stretch

We analyzed the proliferation of rat VSMCs by counting cell numbers (**Fig. 6B**). Static stretch of 25% for 10 min significantly increased the cell number compared with non-stretch (25% static stretch: $3.34 \times 10^5 \pm 13{,}000$ vs. non-stretch: $2.92 \times 10^5 \pm 21{,}500$, $p < 0.0001$). At 48 h without stretch, there is no significant difference in the cell number of VSMCs transfected with control-siRNA and clusterin-siRNA (clusterin-siRNA: $2.72 \times 10^5 \pm 15{,}500$ vs. control-siRNA: $2.92 \times 10^5 \pm 21{,}500$). In contrast, at 48 h after stretching, the cell number of VSMCs treated with clusterin-siRNA was significantly lower than VSMCs treated with control-siRNA (clusterin-siRNA: $2.68 \times 10^5 \pm 40{,}600$ vs. control-siRNA: $3.34 \times 10^5 \pm 13{,}000$, $p < 0.001$).

Clusterin-siRNA Upregulates p53 and p21 After Stretching

We analyzed the expressions of clusterin, p53 and p21 at 48 h after 25% static stretch for 10 min. Western blotting showed that treatment of rat VSMCs cultured with clusterin-siRNA decreased the expression of clusterin and upregulated the expression of p53 and p21 compared to VSMCs cultured with control-siRNA (**Fig. 6C**).

Discussion

Clusterin has been implicated in various cell functions involved in carcinogenesis and tumor progression, including cell adhesion, tissue remodeling,

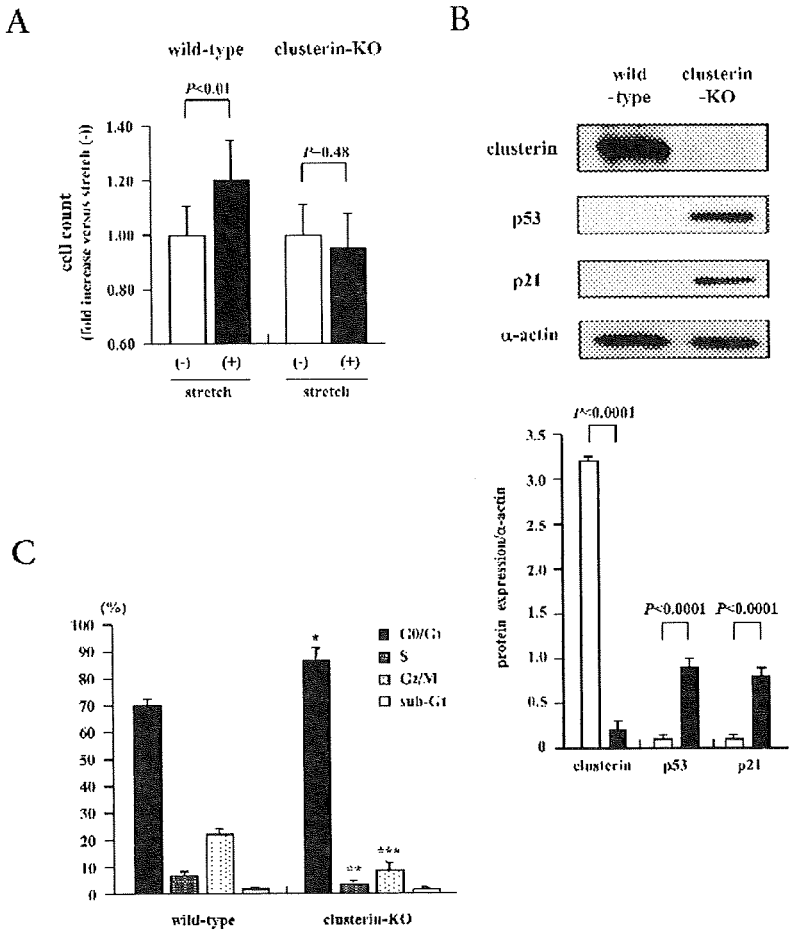

Fig. 5. Induction of p53 and p21, and G1 arrest by stretching in clusterin-KO VSMCs.

The fold increase of cell number after 48 h with (black bar) or without (white bar) 25% stretch for 10 min in wild-type and clusterin-KO VSMCs (A) ($n=6$ per group). Western blotting (B) ($n=3$ replications) and cell cycle analysis by the flow cytometry (C) ($n=4$ times) at 24 h after 25% static stretch for 10 min in wild-type and clusterin-KO VSMCs. $^{*}p<0.00001$ versus wild-type G0/G1, $^{**}p<0.05$ versus wild-type S, $^{***}p<0.00001$ versus wild-type G2/M.

lipid transportation, membrane re-cycling, immune system and cell-cycle regulation, DNA repair, and apoptotic cell death[25]. In addition, clusterin was reported to function as an extracellular chaperone that stabilizes stressed proteins in a folding-competent state[8]. Increased clusterin mRNA and protein levels have been detected in various tissues undergoing stress, including heart, brain, liver, kidney, and retinal tissues both *in vitro* and *in vivo*.

Surprisingly, immunohistochemistry of the injured femoral artery in clusterin-KO mice demonstrated the accumulation of p53 in nuclei of neointimal VSMCs. Moreover, VSMCs from either clusterin-KO or rat VSMCs treated with siRNA that were subjected to static stretch exhibited significantly increased p53 and p21, and increased G1 cell cycle arrest as indicated by flow cytometry compared with wild-type VSMCs. Previous studies have reported that p53 acts as a transcriptional repressor of the clusterin gene[26, 27]; however, we could not determine the precise molecular mechanism by which the inhibition of clusterin expression led to upregulation of p53. Both clusterin and p53 limit tissue injury and/or promote tissue remodeling; therefore, we speculate that p53 may be upregulated in order to compensate for the deficiency of clusterin in tissue damage or tissue

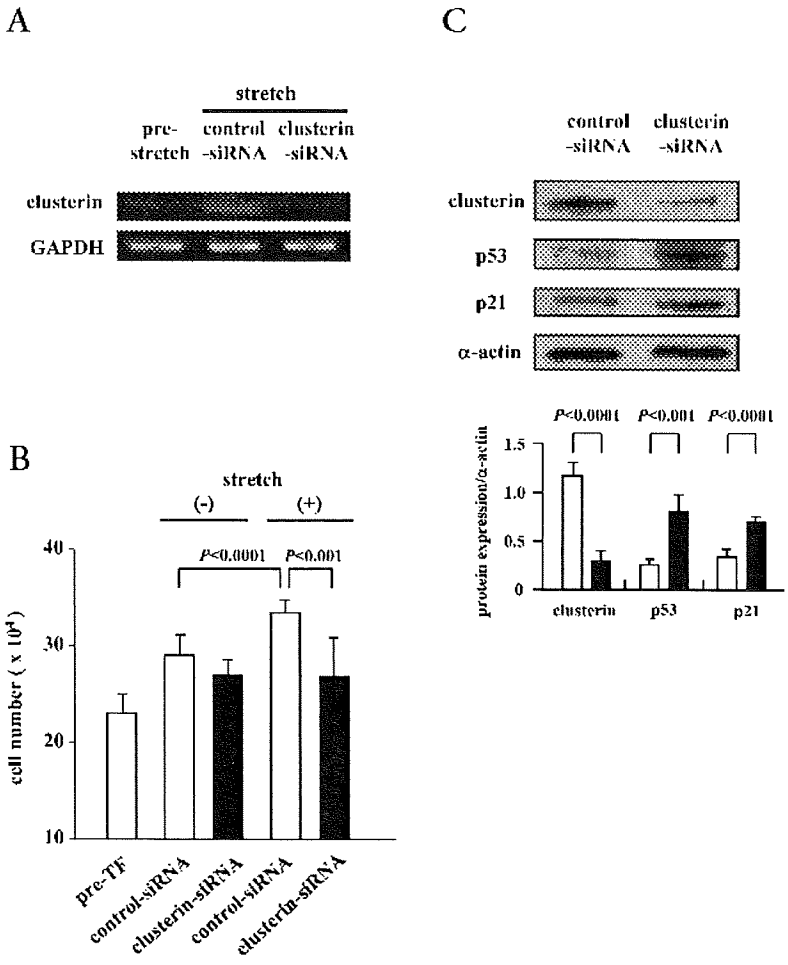

Fig. 6. Clusterin-siRNA decreased VSMC proliferation and upregulated p53 and p21 after stretching in rat VSMCs.

RT-PCR demonstrated the induction of clusterin by static stretch and knock down by clusterin-siRNA in rat VSMCs at 24 h after stretching for 10 min (A). 48 h after stretching, clusterin-siRNA decreased VSMC proliferation stimulated by 25% static stretch for 10 min (B) ($n=6$ per group). Western blotting showed that clusterin-siRNA decreased the expression of clusterin and upregulated the expressions of p53 and p21 in cultured rat VSMCs compared with control-siRNA at 48 h after 25% static stretch for 10 min (C) ($n=3$ replications).

remodeling.

The tumor suppressor p53 is a transcription factor which has been identified as a participant in the cellular DNA damage response resulting in either G1 arrest[28, 29] or apoptosis[28, 30, 31]. It is well established that the induction of p53 tumor suppressor protein can lead to either cell-cycle arrest or apoptosis. Several factors, including the cell type, the presence or absence of survival factors in the external environment, the extent of DNA damage, the level of p53 and post-translational modifications, are involved in the choice between cell-cycle arrest and apoptosis[32]. In our experiments using clusterin-KO mice, vascular damage by cuff implantation upregulated p53, suggesting G1 arrest rather than apoptosis.

p53 is an important factor for maintaining genetic stability and is a cell-cycle check-point protein that helps to regulate progression from G1 into S phase. Many environmental insults and cancer treatments, including γ radiation and chemotherapeutic drugs, increase p53 levels, leading to a G1 phase cell-cycle arrest[29-31]. The G1 arrest pathway involves p53-

dependent transcriptional activation of p21[28]. p21 inhibits G1 cyclin-Cdk complex, such as cyclin D-Cdk4/Cdk6 and cyclin E-Cdk2[33]. Inhibition of G1 cyclin-Cdk complex, in turn, inhibits phosphorylation of pRb[33, 34], thereby preventing activation of E2F-responsive G1/S transition genes, such as dihydrofolate reductase and thymidylate synthase[35]. Thus, p53 helps to maintain genetic stability by preventing progression to the S phase under adverse conditions, such as those created by environmental stresses or treatment with anticancer agents[36]. In our *in vitro* experiments, we confirmed that clusterin-KO VSMCs subjected to stretching upregulated p53 and p21, and shifted to G1 arrest compared with wild-type VSMCs.

Clusterin expression has been associated with the progression of various human tumors, including bladder, colon, prostate, breast, lung, kidney, ovary, and lymphoma[25]. The elevated level of clusterin in human cancer may promote oncogenic transformation and tumor progression by interfering with Bax pro-apoptotic activity[37]. Silencing expression of the clusterin gene in human cancer cells using small interfering RNA was reported to induce spontaneous apoptosis, and reduce growth ability and cell sensitization to genotoxic and oxidative stress[9]. In the same way as gene therapy for cancer, silencing the expression of the clusterin gene in coronary arteries after PCI might be useful to prevent restenosis in the clinical setting.

In this study, the mechanism of cell injury is different between cuff placement (*in vivo*) and cell stretch (*in vitro*). Cuff placement induced neointimal formation following injury and inflammation of adventia of the femoral artery. Injury by both cuff placement and cell stretch upregulated the expression of clusterin in VSMCs.

As compared with wild-type mice, clusterin-KO mice demonstrated a significant decrease of neointimal hyperplasia following vascular injury. In addition, VSMCs from either clusterin-KO or rat VSMCs treated with siRNA that were subjected to static stretch exhibited significantly increased p53 and p21, and increased G1 cell-cycle arrest compared with wild-type VSMCs; therefore, clusterin represents a promising molecular target to limit restenosis after PCI.

Ackowledgments

We wish to thank A. Nagaki for technical assistance. This study was supported in part by a Grant-in-aid for Scientific Research from the Japan Society for the Promotion of Science.

References

1) Morice MC, Serruys PW, Sousa JE, Fajadet J, Ban Hayashi E, Perin M, Colombo A, Schuler G, Barragan P, Guagliumi G, Molnàr F, Falotico R; RAVEL Study Group: Randomized study with the Sirolimus-Coated Bx Velocity Balloon-Expandable Stent in the Treatment of Patients with de Novo Native Coronary Artery Lesions A randomized comparison of a sirolimus-eluting stent with a standard stent for coronary revascularization. N Engl J Med, 2002; 346: 1773-1780
2) Stone GW, Ellis SG, Cox DA, Hermiller J, O'Shaughnessy C, Mann JT, Turco M, Caputo R, Bergin P, Greenberg J, Popma JJ, Russel ME; TAXUS-IV Investigators: A polymer-based, paclitaxel-eluting stent in patients with coronary artery disease. N Engl J Med, 2004; 350: 221-231
3) Okayama S, Uemura S, Nishida T, Morikawa Y, Onoue K, Takemoto Y, Soeda T, Somekawa S, Ishigami K, Takeda Y, Horii M, Kawata H, Takaoka M, Nakajima T, Saito Y: Progression of non-culprit coronary artery atherosclerosis after acute myocardial infarction in comparison with stable angina pectoris. J Atheroscler Thromb, 2008; 15: 228-234
4) Babapulle MN, Joseph L, Bélisle P, Brophy JM, Eisenberg MJ: A hierarchical Bayesian meta-analysis of randomized clinical trials of drug-eluting stents. Lancet, 2004; 364: 583-591
5) Ohkawara N, Ueda H, Shinozaki S, Kitajima T, Ito Y, Asaoka H, Kawakami A, Kaneko E, Shimokado K: Hepatocyte growth factor fusion protein having collagen-binding activity (CBD-HGF) accelerates re-endothelialization and intimal hyperplasia in balloon-injured rat carotid artery. J Atheroscler Thromb, 2007; 14: 185-191
6) Miyata M, Biro S, Kaieda H, Eto H, Orihara K, Kihara T, Obata H, Matsushita N, Matsuyama T, Tei C: Apolipoprotein J/Clusterin is induced in vascular smooth muscle cells after vascular injury. Circulation, 2001; 104: 1407-1412
7) Orlandi A, Pucci S, Ciucci A, Pichiorri F, Ferlosio A, Spagnoli LG: Modulation of clusterin isoforms is associated with all-trans retinoic acid-induced proliferative arrest and apoptosis of intimal smooth muscle cells. Arterioscler Thromb Vasc Biol, 2005; 25: 348-353
8) Trougakos IP, Gonos ES: Clusterin/apolipoprotein J in human aging and cancer. Int J Biochem Cell Biol, 2002; 34: 1430-1448
9) Trougakos IP, So A, Jansen B, Gleave ME, Gonos ES: Silencing expression of the clusterin/apolipoprotein J gene in human cancer cells using small interfering RNA induces spontaneous apoptosis, reduced growth ability, and cell sensitization to genotoxic and oxidative stress. Cancer Res, 2004; 64: 1834-1842
10) Shannan B, Seifert M, Leskov K, Willis J, Boothman D, Tilgen W, Reichrath J: Challenge and promise: roles for clusterin in pathogenesis, progression and therapy of cancer. Cell Death Differ, 2006; 13: 12-19
11) McLaughlin L, Zhu G, Mistry M, Ley-Ebert C, Stuart WD, Florio CJ, Groen PA, Witt SA, Kimball TR, Witte DP, Harmony JA, Aronow BJ: Apolipoprotein J/clusterin

limits the severity of murine autoimmune myocarditis. J Clin Invest, 2000; 106: 1105-1113
12) Moroi M, Zhang L, Yasuda T, Virmani R, Gold HK, Fishman MC, Huang PL: Interaction of genetic deficiency of endotherial nitric oxide, gender, and pregnancy in vascular response to injury in mice. J Clin Invest, 1998; 101: 1225-1232
13) Lardenoye JH, Delsing DJ, de Vries MR, Deckers MM, Princen HM, Havekes LM, van Hinsbergh VW, van Bockel JH, Quax PH: Accelerated atherosclerosis by placement of a perivascular cuff and a cholesterol-rich diet in ApoE*3Leiden transgenic mice. Circ Res, 2000; 87: 248-253
14) Miyata M, Biro S, Kaieda H, Tanaka H: Lipoprotein(a) stimulates the proliferation of cultured human arterial smooth muscle cells through two pathways. FEBS Lett, 1995; 377: 493-496
15) Kozai T, Eto M, Yang Z, Shimokawa H, Lücsher TF: Statins prevent pulsatile stretch-induced proliferation of human saphenous vein smooth muscle cells via inhibition of Rho/Rho-kinase pathway. Cardiovasc Res, 2005; 68: 475-482
16) Wung BS, Cheng JJ, Chao YJ, Hsieh HJ, Wang DL: Modulation of Ras/Raf/extracellular signal-regulated kinase pathway by reactive oxygen species is involved in cyclic strain-induced early growth response-1 gene expression in endothelial cells. Circ Res, 1999; 84: 804-812
17) Eto H, Biro S, Miyata M, Kaieda H, Obata H, Kihara T, Orihara K, Tei C: Angiotensin II type 1 receptor participates in extracellular matrix production in the late stage of remodeling after vascular injury. Cardiovasc Res, 2003; 59: 200-211
18) Okamoto H, Fujioka Y, Takahashi A, Takahashi T, Taniguchi T, Ishikawa Y, Yokoyama M: Trichostatin A, an inhibitor of histone deacetylase, inhibits smooth muscle cell proliferation via induction of p21(WAF1). J Atheroscler Thromb, 2006; 13: 183-191
19) Eto H, Miyata M, Kume N, Minami M, Itabe H, Orihara K, Hamasaki S, Biro S, Otsuji Y, Kita T, Tei C: Expression of lectin-like oxidized LDL receptor-1 in smooth muscle cells after vascular injury. Biochem Biophys Res Commun, 2006; 341: 591-598
20) Orihara K, Biro S, Hamasaki S, Eto H, Miyata M, Ikeda Y, Tei C: Hyperthemia at 43 degree C for 2 h inhibits the proliferation of vascular smooth muscle cells, but not endothelial cells. J Mol Cell Cardiol, 2002; 34: 1205-1215
21) Nakaya K, Ayaori M, Hisada T, Sawada S, Tanaka N, Iwamoto N, Ogura M, Yakushiji E, Kusuhara M, Nakamura H, Ohsuzu F: Telmisartan enhances cholesterol efflux from THP-1 macrophages by activating PPARgamma. J Atheroscler Thromb, 2007; 14: 133-141
22) Eto H, Miyata M, Shirasawa T, Akasaki Y, Hamada N, Nagaki A, Orihara K, Biro S, Tei C: The long-term effect of angiotensin II type 1a receptor deficiency on hypercholesterolemia-induced atherosclerosis. Hypertens Res, 2008; 31: 1631-1642
23) Michel D, Chatelain G, North S, Brun G: Stress-induced transcription of the clusterin/apoJ gene. Biochem J, 1997; 328: 45-50
24) Akishita M, Horiuchi M, Yamada H, Zhang L, Shirakami G, Tamura K, Ouchi Y, Dzau VJ: Inflammation influences vascular remodeling through AT2 receptor expression and signaling. Physiol Genomics, 2000; 2: 13-20
25) Shannan B, Seifert M, Boothman DA, Tilgen W, Reichrath J: Clusterin and DNA repair: a new function in cancer for a key player in apoptosis and cell cycle control. J Mol Histol, 2006; 37: 183-188
26) Klokov D, Criswell T, Leskov KS, Araki S, Mayo L, Boothman DA: IR-inducible clusterin gene expression: a protein with potential roles in ionizing radiation-induced adaptive responses, genomic instability, and bystander effects. Mutat Res, 2004; 568: 97-110
27) Criswell T, Klokov D, Beman M, Lavik JP, Boothman DA: Repression of IR-inducible clusterin expression by the p53 tumor suppressor protein. Cancer Biol Ther, 2003; 2: 372-380
28) El-Deiry WS, Harper JW, O'Connor PM, Velculescu VE, Canman CE, Jackman J, Pietenpol JA, Burrell M, Hill DE, Wang Y, Wiman KG, Mercer WE, Kastan MB, Kohn KW, Elledge SJ, Kinzler KW, Vogelstein B: WAF1/CIP1 is induced in p53-mediated G1 arrest and apoptosis. Cancer Res, 1994; 54: 1169-1174
29) Kastan MB, Onyekwere O, Sidransky D, Vogelstein B, Craig RW: Participation of p53 protein in the cellular response to DNA damage. Cancer Res, 1991; 51: 6304-6311
30) Lowe SW, Schmitt EM, Smith SW, Osborne BA, Jacks T: p53 is required for radiation-induced apoptosis in mouse thymocytes. Nature, 1993; 362: 847-849
31) Clarke AR, Purdie CA, Harrison DJ, Morris RG, Bird CC, Hooper ML, Wyllie AH: Thymocyte apoptosis induced by p53-dependent and independent pathways. Nature, 1993; 362: 849-852
32) Liebermann DA, Hoffman B, Vesely D: p53 induced growth arrest versus apoptosis and its modulation by survival cytokines. Cell Cycle, 2007; 6: 166-170
33) Harper JW, Adami GR, Wei N, Keyomarsi K, Elledge SJ: The p21 Cdk-interacting protein Cip1 is a potent inhibitor of G1 cyclin-dependent kinases. Cell, 1993; 75: 805-816
34) Dulić V, Kaufmann WK, Wilson SJ, Tlsty TD, Lees E, Harper JW, Elledge SJ, Reed SI: p53-dependent inhibition of cyclin-dependent kinase activities in human fibroblasts during radiation-induced G1 arrest. Cell, 1994; 76: 1013-1023
35) Farnham PJ, Slansky JE, Kollmar R: The role of E2F in the mammalian cell cycle. Biochim Biophys Acta, 1993; 1155: 125-131
36) Linke SP, Clarkin KC, Di Leonardo A, Tsou A, Wahl GM: A reversible, p53-dependent G0/G1 cell cycle arrest induced by ribonucleotide depletion in the absence of detectable DNA damage. Genes Dev, 1996; 10: 934-947
37) Zhang H, Kim JK, Edwards CA, Xu Z, Taichman R, Wang CY: Clusterin inhibits apoptosis by interacting with activated Bax. Nat Cell Biol, 2005; 7: 909-915

Original Article

Association between Arterial Stiffness and Estimated Glomerular Filtration Rate in the Japanese General Population

Takuro Kubozono[1], Masaaki Miyata[1], Kiyo Ueyama[1], Aya Nagaki[1], Shuichi Hamasaki[1], Ken Kusano[2], Osamu Kubozono[2], and Chuwa Tei[1]

[1]Department of Cardiovascular, Respiratory and Metabolic Medicine, Graduate School of Medicine, Kagoshima University, Kagoshima, Japan
[2]JA Kagoshima Kouseiren Medical Health Care Center, Kagoshima, Japan

Aim: Chronic kidney disease (CKD) is associated with an increased risk of cardiovascular disease, although it has yet to be established whether CKD is an independent risk factor for arterial stiffness in community residents. The purpose of this study was to determine the correlation between the cardio-ankle vascular index (CAVI) and estimated glomerular filtration rate (eGFR) in the general population.
Methods: We studied 881 consecutively enrolled subjects undergoing health checkups. CAVI was calculated automatically from the pulse volume record, blood pressure and the vascular length from the heart to the ankle. CKD was evaluated by the eGFR.
Results: The distribution of eGFR was as follows: 241 with eGFR (mL/min/1.73m^2) ≥90; 572 with eGFR 60–89; 65 with eGFR 30–59; 3 with eGFR 15–29; 0 with eGFR <15. Linear regression analysis showed that CAVI was negatively correlated significantly with eGFR, while multiple regression analysis using CAVI as an objective variable, adjusted for conventional atherosclerotic risk factors and eGFR as explanatory variables, demonstrated that CAVI was an independent determinant of eGFR. We also showed that stepwise increments of CAVI occurred with progressive deterioration of CKD.
Conclusion: CAVI was independently correlated with eGFR indicating that CKD is associated with arterial stiffness in the general population.

J Atheroscler Thromb, 2009; 16:840-845.

Key words; Cardio-ankle vascular index, Chronic kidney disease, Arterial stiffness

Introduction

Chronic kidney disease (CKD) is a worldwide public health problem[1]. Cardiovascular disease (CVD) is associated frequently with CKD, a relationship that is important given that individuals with CKD are more likely to die of CVD than to develop kidney failure[2]. Numerous studies have established that CKD is a major risk factor for CVD, not only in populations at high risk for CVD, but also in the general population[3-5]. It has been reported that microalbuminuria is a strong determinant of ischemic heart disease and death, independent of age, sex, hypertension, diabetes mellitus, renal function and the plasma lipid profile[6]. As a consequence, mild renal dysfunction has recently attracted increased attention, with a reduction in the estimated glomerular filtration rate (eGFR) being regarded as a useful index of kidney damage and also an effective strategy for detecting patients with CKD[7].

Recently, an atherosclerotic index, the cardio-ankle vascular index (CAVI), has been developed that involves measuring pulse wave velocity (PWV) and blood pressure (BP). CAVI is adjusted for BP based on the stiffness parameter β and is expressed as arterial stiffness independent of BP[8, 9]. We have reported previously that CAVI showed a weaker correlation

Address for correspondence: Masaaki Miyata, Department of Cardiovascular, Respiratory and Metabolic Medicine, Graduate School of Medicine, Kagoshima University, 8-35-1 Sakuragaoka, Kagoshima 890-8520, Japan
E-mail: miyatam@m3.kufm.kagoshima-u.ac.jp
Received: December 10, 2008
Accepted for publication: June 11, 2009

with systolic BP (SBP) than with brachial-ankle PWV (baPWV) and was not affected by changes in BP during measurement[9]. There is also evidence that CAVI is associated significantly with the presence and severity of coronary atherosclerosis[10].

While it has been reported that PWV correlates negatively with eGFR in community residents[11], it has not yet been determined whether CAVI correlates with eGFR in the general population. The purpose of this study was therefore to determine the correlation between CAVI and eGFR in the general Japanese population.

Methods

Subjects

The study group consisted of 881 consecutively enrolled subjects (488 males and 393 females, mean age: 52 ± 14 years, range: 18–80 years) who underwent routine health checkups at JA Kagoshima Kouseiren Medical Health Care Center. Personal interviews showed that 112 subjects were receiving treatment for hypertension, 10 for diabetes mellitus and 36 for hyperlipidemia. Five subjects had a history of ischemic heart disease and 10 had a history of stroke. Information on smoking history was obtained by means of a self-administered questionnaire.

The protocol used for the present study was approved by the institutional review board of Kagoshima University. Informed consent was obtained from all volunteers.

Biochemical Measurements

Blood samples were collected after the subjects had fasted overnight. The serum concentrations of total cholesterol (TC), triglyceride (TG) and high density lipoprotein (HDL)-cholesterol were measured by standard laboratory procedures, while low density lipoprotein (LDL)-cholesterol was calculated by the Friedewald equation. Eight subjects with a serum TG concentration of 400 mg/dL or higher did not have their LDL-cholesterol calculated as the Friedewald equation is unsuitable for TG values above this level.

Measurements of Proteinuria

Dipstick urinalysis for proteinuria was performed on spontaneously voided fresh urine samples. The test results were interpreted by physicians and recorded as −, ±, 1+, 2+, 3+ or 4+. Results recorded as − and ± were classified as the absence of proteinuria and the others were classified as the presence of proteinuria.

Measurements of Estimated GFR

CKD was evaluated by eGFR using the equation of the Japanese Society of Nephrology: $eGFR = 194 \times Cr^{-1.094} \times age^{-0.287}$ (mL/min/1.73 m^2). For women, the eGFR was multiplied by a correction factor of 0.739. eGFR was classified using the following five categories provided by the Kidney Disease Outcomes Quality Initiative (K/DOQI)[12]: stage 1: eGFR ≥90 mL/min/1.73 m^2; stage 2: eGFR 60 to 89 mL/min/1.73 m^2; stage 3: eGFR 30 to 59 mL/min/1.73 m^2; stage 4: eGFR 15 to 29 mL/min/1.73 m^2; stage 5 eGFR < 15 mL/min/1.73 m^2. In 2002, the National Kidney Foundation published clinical practice guidelines on evaluation, classification and risk stratification in CKD. In these guidelines, CKD is defined as either kidney damage for ≥3 months, as confirmed by kidney biopsy or markers of kidney damage, with or without a decrease in GFR; or GFR < 60 mL/min/1.73 m^2 for ≥3 months, with or without kidney damage[12].

Measurements of CAVI

CAVI was measured using a Vasera VS-1000 (Fukuda Denshi, Tokyo, Japan) as reported previously[8-10]. Briefly, cuffs were applied to the four extremities and electrocardiographic electrodes were attached to the upper arm. A microphone was placed on the sternal angle for phonocardiography. The subjects then rested in the supine position for 5 min. PWV was calculated by dividing the distance from the aortic valve to the ankle artery by the sum of the difference between the time the pulse waves were transmitted to the brachium and the time the same waves were transmitted to the ankle, and the time difference between the second heart sound on the phonocardiogram and the notch of the brachial pulse waves[9]. To minimize cuff inflation effects on blood flow dynamics, pulse waves were measured with the cuffs inflated to lower than diastolic BP (DBP) (50 mmHg). Extremity blood pressure was then measured by oscillometry. SBP, DBP and pulse pressure (PP) were obtained by measuring blood pressure at the right brachial artery. In this study, there were no patients with peripheral artery disease with an ankle brachial index less than 0.9.

CAVI was calculated by the following equation: $CAVI = a\ [\{2\rho \times 1/(SBP-DBP)\} \times \{\ln (SBP/DBP) \times PWV^2\}] + b$ (ρ: density of blood, a and b: constants)[9, 10, 13].

Statistical Analysis

Data are expressed as the mean ± SD. Differences between the mean values of the two groups were analyzed by unpaired *t* tests. The relationship between

Table 1. Characteristics of the subjects

Variable	(n=881)
Age (years)	52±14
BMI (kg/m^2)	23.0±3.3
Gender (male/female)	488/393
Triglycerides (mg/dL)	110±73
HDL cholesterol (mg/dL)	58±15
LDL cholesterol (mg/dL)	124±30
FBS (mg/dL)	103±21
Hemoglobin A1c (%)	5.2±0.6
BUN (mg/dL)	15.4±4.2
Creatinine (mg/dL)	0.7±0.2
Systolic BP (mmHg)	127±17
Diastolic BP (mmHg)	82±12
Mean BP (mmHg)	99±15
Pulse pressure (mmHg)	45±10
Smoking history (%)	50
eGFR (ml/min/1.73 m^2)	81±16
CAVI	8.5±1.3

BMI, body mass index; HDL, high density lipoprotein; LDL, low density lipoprotein; FBS, fasting blood sugar; BUN, blood urea nitrogen; BP, blood pressure; eGFR, estimated glomerular filtration rate; CAVI, cardio-ankle vascular index.

continuous variables was analyzed by linear regression analysis. The independence of the association between variables was tested with multiple regression analysis. Statistical analyses were performed with Stat View, version 5.0. P values less than 0.05 were considered significant.

Results

Background of Subjects

The clinical characteristics of the subjects are summarized in **Table 1**. The mean age was 52±14 years (range, 18 to 80 years). The mean value of eGFR was 81±16 mL/min/1.73 m^2, with the distribution of eGFR and CKD stages as follows: stage 1, n=241; stage 2, n=572; stage 3, n=65; stage 4, n=3; stage 5, n=0. The mean value of CAVI was 8.5±1.3.

Relationship between CAVI and Risk Factors

Linear regression analysis showed that CAVI correlated significantly with age, LDL cholesterol, TG, HDL cholesterol, FBS, HbA1c, BUN, serum creatinine, SBP, DBP and PP (**Table 2**). In addition, there was a significant negative correlation between CAVI and eGFR (**Fig. 1**).

Table 2. Linear regression analysis between CAVI and other variables

Variable	r	p value
Age	0.699	<0.0001
BMI	0.025	0.47
Triglycerides	0.131	<0.0001
HDL cholesterol	−0.114	<0.001
LDL cholesterol	0.155	<0.0001
FBS	0.247	<0.0001
Hemoglobin A1c	0.196	<0.0001
BUN	0.308	<0.0001
Creatinine	0.170	<0.0001
Systolic BP	0.402	<0.0001
Diastolic BP	0.359	<0.0001
Mean BP	0.443	<0.0001
Pulse pressure	0.266	<0.0001
eGFR	−0.383	<0.0001

BMI, body mass index; HDL, high density lipoprotein; LDL, low density lipoprotein; FBS, fasting blood sugar; BUN, blood uria nitrogen; BP, blood pressure; eGFR, estimated glomerular filtration rate.

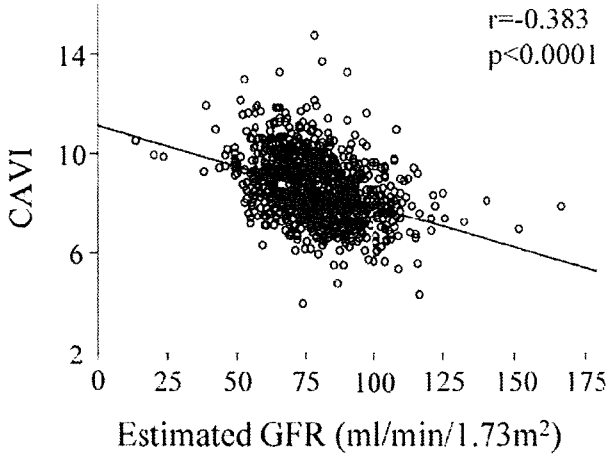

Fig. 1. Relationship between CAVI and eGFR in the general population.

CAVI, cardio-ankle vascular index; eGFR, estimated glomerular filtration rate.

Multiple Regression Analysis between CAVI and Other Clinical Variables

Multiple regression analysis was performed using CAVI as an objective variable, adjusted for conventional atherosclerotic risk factors that included age, gender, SBP, LDL cholesterol, hemoglobin A1c and eGFR, as explanatory variables. This analysis demonstrated that CAVI correlated independently with age, hemoglobin A1c, SBP, history of smoking and eGFR